Supporting Information

Porous nanosheets of Cu₃P@N, P co-doped carbon hosted on copper foam as an efficient and ultrastable pH-universal hydrogen evolution electrocatalyst

Enjun Jiang[‡a], Jianhong Jiang[‡b], Guo Huang[a], Zhiyi Pan[a], Xiyong Chen[a], Guifang Wang[a], Shaojian Ma[a], Jinliang Zhu*[a] and Pei Kang Shen[a]

[a] *Guangxi Key Laboratory of Processing for Non-ferrous Metals and Featured Materials, School of Resources, Environment and Materials, Collaborative Innovation Center of Sustainable Energy Materials, Guangxi University, 100 Daxue Dong Road, Nanning 530004, PR China.*
[b] *College of Chemistry Biology and Environmental Engineering, Xiangnan University, Chenzhou, 423043, China*

‡ *These authors contributed equally.*

Corresponding authors: Email: jlzhu85@163.com (Jinliang Zhu)

Experimental Section

Synthesis of Cu₃P@NPC-CF

Clear copper foam (6 × 3 × 0.15 cm) was covered on a corundum boat containing 1.8 g of phosphoramidic acid resin (Shanghai Xrun Resin Co., Ltd, China). The corundum boat was placed in a tube furnace and the temperature raised to 900 °C at a rate of 5 °C per minute, and then maintained at this temperature for 1 hour under a N_2 atmosphere. After cooling to 30 °C, porous nanosheets of N, P co-doped carbon wrapped in Cu_3P, grown on the copper foam were obtained and noted as Cu₃P@NPC-CF. For comparision, N, P co-doped carbon (NPC) was synthesized under the same condition without the copper foam.

Physical characterization

The morphology of the catalyst was analyzed by field-emission scanning electron microscopy (SEM, SU8220, Hitachi Corp., Japan), atomic force microscope (Bruker, USA) and transmission electron microscope (TEM, Tian ETEM G2 80-300, FEI Corp., USA). The X-ray diffraction pattern was tested by D/Max-III Diffractometer (Rigaku Corporation, Japan) from 20-80° with a scanning speed of 6° min^{-1}. X-ray photoelectron spectroscopy (XPS, ESCALab 250Xi, Thermo Fisher Scientific, USA; Al Kα) was used to analyze the elemental composition, electronic structure and chemical state of the material surface. The specific surface area and pore size distributions were calculated by the N_2 isothermal adsorption/desorption curves at 77 K.

Electrochemical Characterization

Electrochemical performance tests were performed on an electrochemical workstation (Zahner IM6e, Germany). In a three-electrode system, Cu₃P@NPC-CF served as the working electrode, whilst a graphite rod and a reversible hydrogen electrode (RHE) served as the counter electrode and reference electrode, respectively. The polarization curves were obtained by linear scanning voltammetry (LSV) with a scanning range of 0.1 to -0.8 V vs. RHE and a scanning speed of 5 mV s^{-1} in 0.5 M H_2SO_4 (pH=0), 1 M PBS (pH=7), and 1 M KOH (pH=14), respectively. Electrochemical impedance spectroscopy (EIS) was conducted between 100 kHz and 100 mHz. The electrochemically surface area (ECSA) was characterized by dual layer capacitance (C_{dl}) which was obtained by CV from 1.2 to 1.25 V vs. RHE at different scanning speeds.
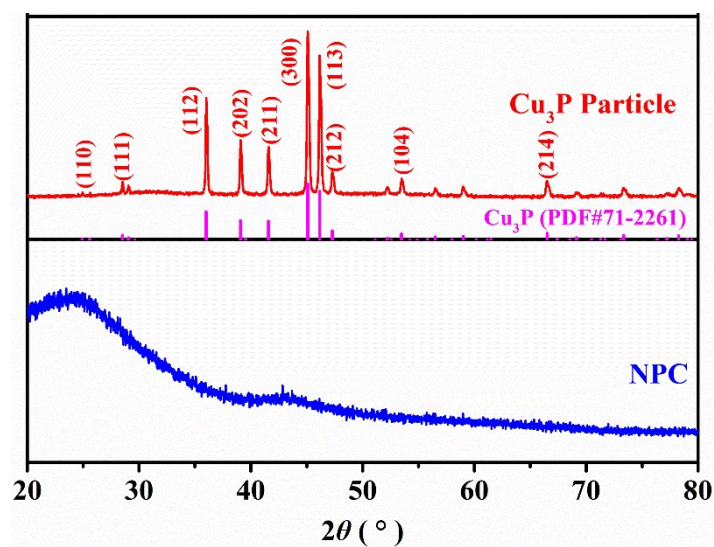
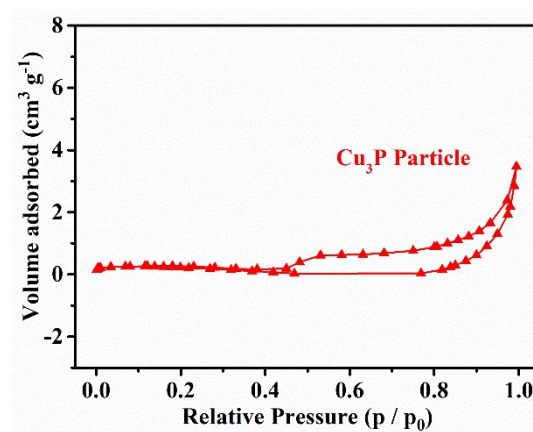**Fig. S1** XRD pattern of Cu$_3$P particle and NPC.
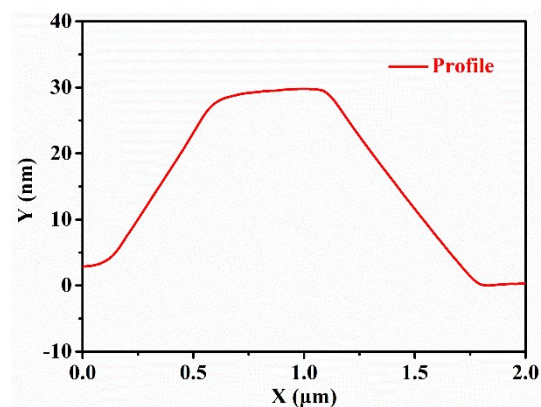

Fig. S2 N$_2$ adsorption/desorption isotherm Cu$_3$P particle.

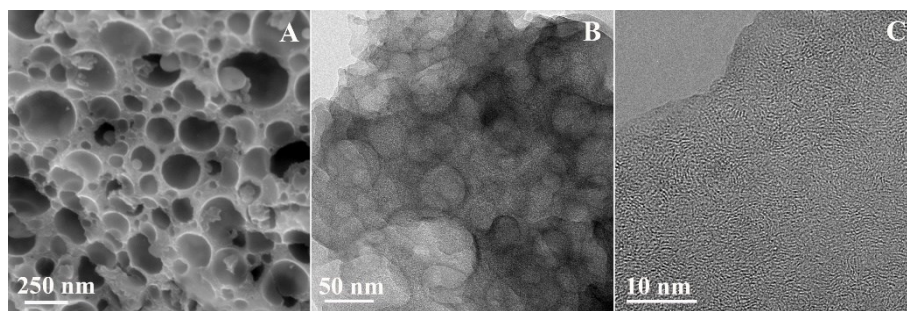**Fig. S3** The height profile of Cu$_3$P@NPC-CF

Fig. S4 (A) SEM image, (B) TEM image, and (C) HRTEM image of NPC.

The SEM and TEM images (**Fig. S4A and B**) show that the NPC possess a porous structure.
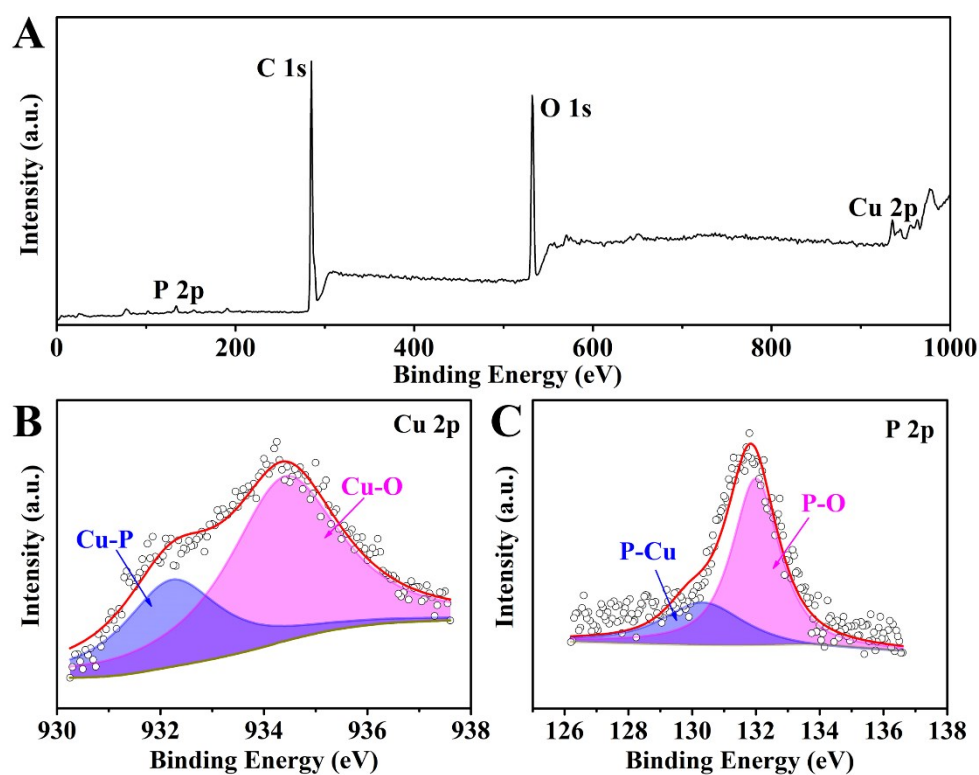

Fig. S5 (A) Survey XPS spectra, high-resolution XPS spectra of (B) Cu 2p, (C) P 2p for Cu_3P particle.

Fig. S6 (A) Survey XPS spectra, high-resolution XPS spectra of (B) C 1s, (C) P 2p, (D) N 1s for NPC.

Fig. S7 (A) TEM, and (B) HRTEM image of Cu$_3$P@NPC-CF after continuous potential cycling in 1 M KOH.

Fig. S8 CV curves of (A) Cu₃P@NPC-CF, (B) Cu₃P particle and (C) NPC with different scan rates. (D) The C_{dl} of Cu₃P@NPC-CF, Cu₃P particle, and NPC.

Fig. S9 Nyquist plots of Cu₃P@NPC-CF and Cu₃P particle for HER with a test voltage of -0.2 V.

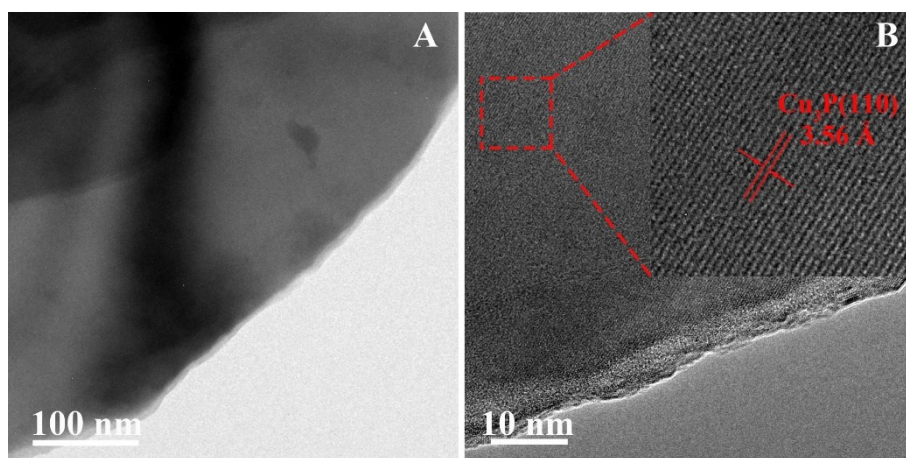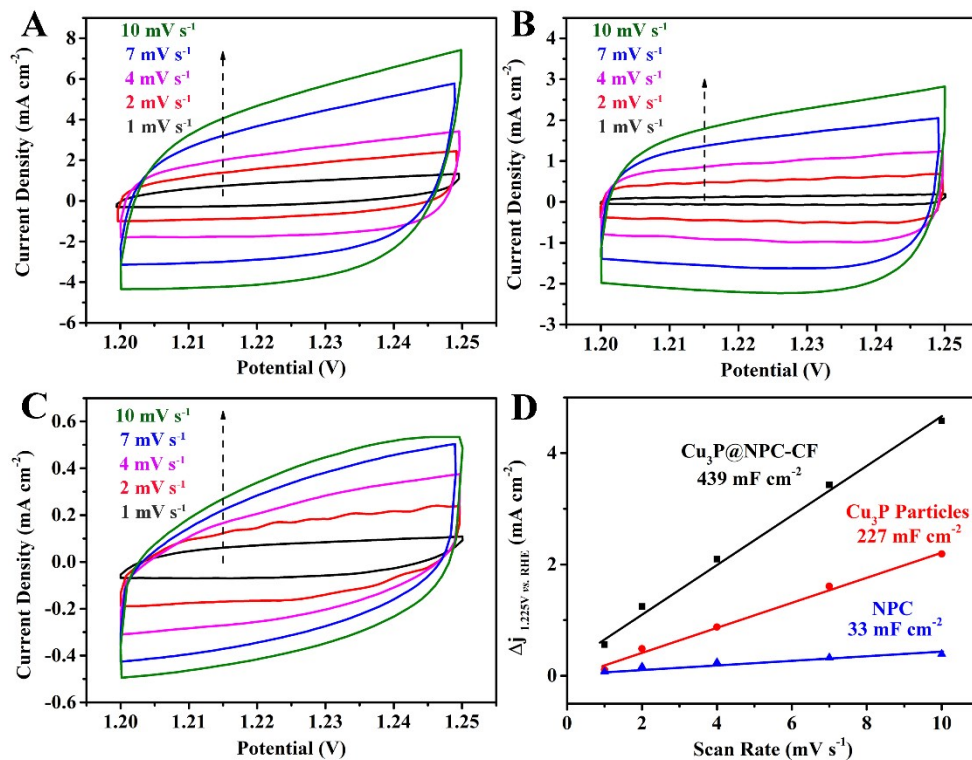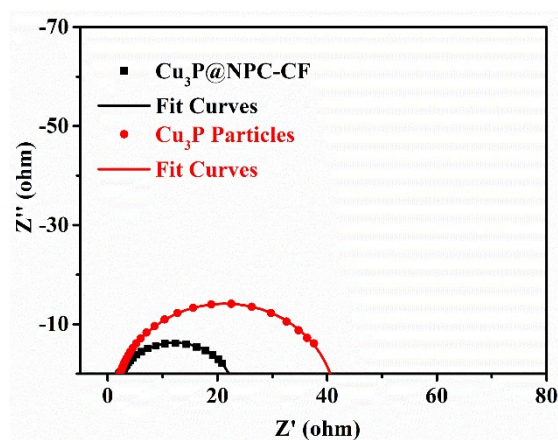**Table S1** Comparison of $Cu_3P@NPC$-CF and catalysts reported for HER in 0.5 M H_2SO_4.

Catalysts	Tafel (mV dec^{-1})	η_{10} (mV)	Stability test (h)	Current retention rate	Ref.
$Cu_3P@NPC$-CF	81.25	81.94	90	81.32%	This Work
$Ni_{0.25}Cu_{0.75}$/C	84	184	20000 s	99%	[S1]
$Ni_{0.85}Se@NC$	85	131	10	99.8%	[S2]
PdNi NWs	96	91	1000 cycles	---	[S3]
$Cu@MoS_2$	51	131	~7	---	[S4]
Cu_3P NW/CF	67	143	25	---	[S5]
NC-CF-PSFN	90.2	124	10	---	[S6]
a-C/$Cu_3P@$ 400 ℃	72	287	1000 cycles	-	[S7]
Broom-like $CuGeO_3$	98	135	80	---	[S8]
Cuf@Ni_5P_4	49	90	84	CP	[S9]
$Ni_3Cu_1@NG$-NC	84.2	122	80	CP	[S10]
$Fe_xP@NPC$	81	227	11	CP	[S11]
$CoP_3/CoMoP$-5/NF	66.1	125	20	---	[S12]
Cu−Co−P	59	262	72	CP	[S13]

Table S2 Comparison of $Cu_3P@NPC-CF$ and catalysts reported for HER in 1 M PBS.

Catalysts	Tafel (mV dec^{-1})	η_{10}(mV)	Stability test (h)	Current retention rate	Ref.
$Cu_3P@NPC-CF$	123.71	192.52	90	96.06%	This Work
Mo-WC@NCS	95	221	12	CP	[S14]
$Er_2Si_2O_7:IrO_{2-5}$	67	190	~4	---	[S15]
CoP/NCNT-CP	100	305	10	CP	[S16]
$CoO/CoSe_2$	131	337	9	---	[S17]
Fe-Co_9S_8 NSs/C	126.9	192	20	---	[S18]
$NiFe_2O_4$/NF	81.3	197	24	---	[S19]
$Ni_3N@Ni–Bi$ NS/Ti	190	265	20	---	[S20]
CuS@C	-	399	1000 cycles	-	[S21]
Co-B	75	251	44	---	[S22]
Ni-Mo-S/C (1:1)	85.3	200	30000 s	97.5%	[S23]

Table S3 Comparison of $Cu_3P@NPC\text{-}CF$ and catalysts reported for HER in 1 M KOH.

Catalysts	Tafel (mV dec^{-1})	η_{10} (mV)	Stability test (h)	Current retention rate	Ref.
$Cu_3P@NPC\text{-}CF$	93.14	135.45	90	95.61%	This Work
NiCoP/SCW	64.4	178	36	83.3%	[S24]
$Cu_{0.50}Fe_{0.50}$/NF	62.18	158	100	CP	[S25]
CuCoO-NWs	108	140	50	---	[S26]
Cu_3N/NF	122	118	14	---	[S27]
Cu−Co−P	86	231	72	CP	[S13]
Ni_3P MPs	119	291	16	CP	[S28]
CoP@FeCoP/NC	47.98	141	20	CP	[S29]
$CuCo_2S_4/NiCo_2S_4$	90	206	15	CP	[S30]
Ni-Co-P/NF	108.4	156	20	---	[S31]
Co/CoP HNC	105.6	180	10	CP (add ~30%)	[S32]

References

S1.   M. A. Ahsan, A. R. Puente Santiago, Y. Hong, N. Zhang, M. Cano, E. Rodriguez-Castellon, L. Echegoyen, S. T. Sreenivasan and J. C. Noveron, *J. Am. Chem. Soc.*, 2020, **142**, 14688-14701.

S2.   Z. Huang, B. Xu, Z. Li, J. Ren, H. Mei, Z. Liu, D. Xie, H. Zhang, F. Dai, R. Wang and D. Sun, *Small*, 2020, **16**, 2004231.

S3.   L. Du, D. Feng, X. Xing, C. Wang, G. S. Armatas and D. Yang, *Chem. Eng.J.*, 2020, **400**, 125864.

S4.   L. Ji, P. Yan, C. Zhu, C. Ma, W. Wu, C. Wei, Y. Shen, S. Chu, J. Wang, Y. Du, J. Chen, X. Yang and Q. Xu, *Appl. Catal. B-Environ.*, 2019, **251**, 87-93.

S5.   J. Tian, Q. Liu, N. Cheng, A. M. Asiri and X. Sun, *Angew. Chem. Int. Ed.*, 2014, **53**, 9577-9581.

S6.   X. Liu, L. Yang, Z. Zhou, L. Zeng, H. Liu, Y. Deng, J. Yu, C. Yang and W. Zhou, *Chem. Eng.J.*, 2020, **399**, 125779.

S7.   A. Manikandan, P. Sriram, K.-C. Hsu, Y.-C. Wang, C.-W. Chen, Y.-C. Shih, T.-J. Yen, H.-T. Jeng, H.-C. Kuo and Y.-L. Chueh, *Electrochim. Acta*, 2019, **318**, 374-383.

S8.   Y. Xiao, B. Li, L. Qin, H. Lin, Q. Li, M. Nie, Y. Li and B. Liao, *Catal. Commun.*, 2020, **144**, 106075.

S9.   M. Das, N. Jena, T. Purkait, N. Kamboj, A. De Sarkar and R. S. Dey, *J. Mater. Chem. A*, 2019, **7**, 23989-23999.

S10.   B. Liu, H. Q. Peng, J. Cheng, K. Zhang, D. Chen, D. Shen, S. Wu, T. Jiao, X. Kong, Q. Gao, S. Bu, C. S. Lee and W. Zhang, *Small*, 2019, **15**, 1901545.

S11.   Y. Cheng, J. Guo, Y. Huang, Z. Liao and Z. Xiang, *Nano Energy*, 2017, **35**, 115-120.

S12.   D. Jiang, Y. Xu, R. Yang, D. Li, S. Meng and M. Chen, *ACS Sustainable Chem. Eng.*, 2019, **7**, 9309-9317.

S13.   R. N. Wasalathanthri, S. Jeffrey, R. A. Awni, K. Sun and D. M. Giolando, *ACS Sustainable Chem. Eng.*, 2018, **7**, 3092-3100.

S14.   L. Wang, Z. Li, K. Wang, Q. Dai, C. Lei, B. Yang, Q. Zhang, L. Lei, M. K. H. Leung and Y. Hou, *Nano Energy*, 2020, **74**, 104850.

S15.   P. Karfa, K. C. Majhi and R. Madhuri, *ACS Catal.*, 2018, **8**, 8830-8843.

S16.   L. Wang, J. Cao, X. Cheng, C. Lei, Q. Dai, B. Yang, Z. Li, M. A. Younis, L. Lei, Y. Hou and K. Ostrikov, *ACS Sustainable Chem. Eng.*, 2019, **7**, 10044-10051.

S17.   K. Li, J. Zhang, R. Wu, Y. Yu and B. Zhang, *Adv Sci (Weinh)*, 2016, **3**, 1500426.

S18.   K. Ao, D. Li, Y. Yao, P. Lv, Y. Cai and Q. Wei, *Electrochim. Acta*, 2018, **264**, 157-165.

S19.   J. Liu, D. Zhu, T. Ling, A. Vasileff and S.-Z. Qiao, *Nano Energy*, 2017, **40**, 264-273.

S20.   L. Xie, F. Qu, Z. Liu, X. Ren, S. Hao, R. Ge, G. Du, A. M. Asiri, X. Sun and L. Chen, *J. Mater. Chem. A*, 2017, **5**, 7806-7810.

S21.   J. Rong, J. Xu, F. Qiu, Y. Fang, T. Zhang and Y. Zhu, *Electrochim. Acta*, 2019, **323**, 134856.

S22.   S. Gupta, N. Patel, A. Miotello and D. C. Kothari, *J. Power Sources*, 2015, **279**, 620-625.

S23.   J. Miao, F.-X. Xiao, H. B. Yang, S. Y. Khoo, J. Chen, Z. Fan, Y.-Y. Hsu, H. M. Chen, H. Zhang and B. Liu, *Sci. Adv.*, 2015, **1**, 1500259.

S24.   V. R. Jothi, R. Bose, H. Rajan, C. Jung and S. C. Yi, *Adv. Energy Mater.*, 2018, **8**, 1802615.

S25.   A. I. Inamdar, H. S. Chavan, B. Hou, C. H. Lee, S. U. Lee, S. Cha, H. Kim and H. Im, *Small*, 2020, **16**, 1905884.

S26.   M. Kuang, P. Han, Q. Wang, J. Li and G. Zheng, *Adv. Funct. Mater.*, 2016, **26**, 8555-8561.

S27.   C. Panda, P. W. Menezes, M. Zheng, S. Orthmann and M. Driess, *ACS Energy Lett.*, 2019, **4**, 747-754.

S28.   A. B. Laursen, R. B. Wexler, M. J. Whitaker, E. J. Izett, K. U. D. Calvinho, S. Hwang, R. Rucker, H. Wang, J. Li, E. Garfunkel, M. Greenblatt, A. M. Rappe and G. C. Dismukes, *ACS Catal.*, 2018, **8**, 4408-4419.

S29.   J. Shi, F. Qiu, W. Yuan, M. Guo and Z.-H. Lu, *Chem. Eng.J.*, 2021, **403**, 126312.

S30.   L. Ma, J. Liang, T. Chen, Y. Liu, S. Li and G. Fang, *Electrochim. Acta*, 2019, **326**, 135002.

S31.   Y. Gong, Z. Xu, H. Pan, Y. Lin, Z. Yang and J. Wang, *J. Mater. Chem. A*, 2018, **6**, 12506-12514.

S32.   Y. Hao, Y. Xu, W. Liu and X. Sun, *Mater. Horizons*, 2018, **5**, 108-115.